

## SUPPLEMENTARY MATERIALS

### Neural Underpinnings of Informational Cascades: Brain Mechanisms of Social Influence On Belief Updating

Rafael E. Huber, Vasily Klucharev, and Jörg Rieskamp

#### I. Supplementary methods - Model estimation

To estimate the free parameters of the three computational models, we applied a Bayesian hierarchical approach (Kruschke, 2011) implemented with the OpenBugs software (Lunn *et al.*, 2009) and the BRugs package (Thomas *et al.*, 2006) in R (R Development Core Team, 2011). All three models provide a point estimate for the posterior probability that one stock is better than the other stock. To compare the model predictions  $\hat{Y}$  (see Equation 3) with the observed probability judgments of the participants, we first transformed the observed probabilities using a logit transformation. We then assumed a normal distributed error ( $\sigma_n$ ) around  $\hat{Y}$  for each participant  $n$  as an additional free parameter. The model parameters for the  $n^{th}$  participant ( $\beta_{0n}$ ,  $\beta_{tn}$  and  $\sigma_n$ ) were sampled from group distributions, whereas the parameters of these group distributions were sampled from higher order distributions. In our hierarchical model, explicit prior assumptions were specified at the top of the hierarchical model only, as all the downstream parameters were connected to the overarching values. The model parameters of interest for the  $n^{th}$  individual (that is,  $\beta_{tn}$  and  $\beta_{0n}$ ) were sampled from normal (group) distributions with means  $M_t$  and  $M_0$  and precisions  $T_t$  and  $T_0$  (where  $SD = 1/\sqrt{T}$ ). The means  $M_t$  and  $M_0$  were sampled from normal hyperparameter distributions with a prior mean of  $\mu_t = 1$  and a precision  $\tau_t = 0.01$  for all  $M_t$  and  $\mu_0 = 0$  and  $\tau_0 = 0.01$  for  $M_0$  (notice that the chosen prior means  $\mu_t$  and  $\mu_0$  represent the normative solution). The precisions  $T_t$  and  $T_0$  were sampled from gamma distributions with Shape = 0.1 and Rate =

0.1. As prior distribution for the error component  $\sigma_n$  we defined a gamma distribution with parameters S and R, which were also sampled from hyperparameter distributions (see Kruschke (2011, p.443) for a detailed description). For an efficient estimation process, we used a thinning factor of 100 and an initial burn-in of 10,000. All final Markov chains had a length of 100,000.

### **Model comparison**

To compare the models we estimated the Deviance Information Criterion (DIC) for all three computational models. The DIC is especially suited to hierarchical models, as it takes the goodness-of-fit and the effective number of free parameters into account. The model with the lowest DIC should predict a replicate data set best (Spiegelhalter *et al.*, 2002).

Additionally, we compared the FM with the SM on the individual level via approximate Bayes factors based on the best fitting parameters (modes of the marginal posterior distributions) using the Bayesian Information Criterion (see Raftery, 1995; Wagenmakers, 2007).

### **Functional imaging data acquisition**

Functional MRI was performed with ascending slice acquisition using a T2\*-weighted echo-planar imaging sequence using a 3T Siemens Magnetom Verio whole-body MR unit equipped with a 12-channel head coil; 40 axial slices; volume repetition time (TR), 2.28 s; echo time (TE), 30 ms; 80° flip angle; slice thickness, 3.0 mm; field of view (FoV) read, 228 mm; slice matrix 76×76. For structural MRI, we acquired a T1-weighted MP-RAGE sequence (176 sagittal slices; volume TR, 2.0 s; TE, 3.37 ms; 8° flip angle; slice matrix 256×256; slice thickness, 1.0 mm; no gap; FoV, 256 mm). We preprocessed the fMRI data using SPM8 (Wellcome Trust Center for Neuroimaging, University College London). We applied a slice time correction using the middle image as reference. Preprocessing was continued with spatial

realignment to correct for head movement. T1 images were then co-registered to the mean functional image created in the previous step. This image was segmented into grey matter, white matter, and cerebrospinal fluid (CSF). In a next step, the data were normalized according to the Montreal Neurological Institute (MNI) template and smoothed with a Gaussian smoothing kernel (FWHM = 8 mm). The start of the experimental paradigm was triggered by the 7<sup>th</sup> scanner pulse to account for magnetization equilibration and previous scans were excluded from the final analysis.

## II. Supplementary behavioural results - Control Study

The standard informational cascades paradigm implies a fixed order of *social* followed by *private information*. However, due to the fixed order of the presented information, it could have been that a different weight assigned to the *private information* simply represented an order effect in which the last piece of information is given larger weight (e.g., Hogarth & Einhorn, 1992). Therefore, in order to examine whether indeed the last piece of information was given larger weight, we conducted a control study in which we had an additional condition in which only *private information* was presented. Seventeen participants (mean age = 21.6 years,  $\pm$  1.7 SD, 20-25 years, 6 females) participated in this additional behavioral study that consisted of 60 trials with 8 filler trials, 26 standard trials (*social information I*, *social information II* and *private information*; similar to the fMRI study) and 26 control trials (*private information I*, *private information II* and *private information III*). To explore a potential order effect, we compared the standard and control trials with each other by estimating the SM model. This enabled us to examine whether *private information* is weighted differently as compared to *social information* or whether simply the last piece of information is given larger weight than the preceding information.

The analysis of the standard trials replicated the behavioral results of the fMRI study: A clear trend towards overweighting of *private information* was observed,  $M_{private} - M_{social}$ ,

mode = 0.165, 95% HDI = -0.0316 – 0.394. Importantly, the analysis of the control trials (consisting of *private information* only) did not show overweighting of the last *private information* at the end of the trial: The marginal posterior for  $M_{private\ III}$  (*private information III*; mode = 0.748, 95% HDI = 0.615-0.873) could not be credibly differentiated from the marginal posterior for  $M_{private\ I+II}$  (*private information I & II*, mode = 0.746, 95% HDI of 0.609-0.876), as indicated by the 95% HDI for the contrast  $M_{private\ III} - M_{private\ I+II}$ , mode = -0.005, 95% HDI = -0.189-0.18. The results of the control study, in particular the control condition, showed that the last piece of information is not overweighted due to a recency effect and no order effect was observed. Thus, we can conclude that the larger weight given to *private information* as compared to *social information* in the fMRI study was due to the *private versus social* character of the information.

### **III. Supplementary fMRI results - The effect of subjective uncertainty during decision making**

The probability judgments (i.e. subjective posterior probabilities) provided by the participants are a very direct measure of subjective uncertainty. Additionally, we analyzed the effect of subjective uncertainty on brain activity during decision making (decision time-window). At the end of each trial, participants made a probability judgment about their decision. We found that increased subjective uncertainty activated the bilateral fronto-parietal network, the left fronto-insular cortex and the dorsomedial prefrontal cortex (DMPFC) (Fig. S1 and Table S1). Thus, the brain areas involved into the belief updating by *private information* were also engaged into the final decision-making process.

## REFERENCES

- Hogarth, R.M., Einhorn, H.J. (1992). Order effects in belief updating: The belief-adjustment model. *Cognitive Psychology*, 24, 1–55. Available at:  
<http://www.sciencedirect.com/science/article/pii/001002859290002J>.
- Kruschke, J.K. (2011). *Doing Bayesian data analysis: A tutorial with R and BUGS*. Burlington, MA: Academic Press.
- Lunn, D., Spiegelhalter, D., Thomas, A., Best, N. (2009). The BUGS project: Evolution, critique and future directions. *Statistics in Medicine*, 28, 3049–67. Available at:  
<http://onlinelibrary.wiley.com/doi/10.1002/sim.3680/abstract>.
- Raftery, A.E. (1995). Bayesian model selection in social research. *Sociological Methodology*, 25, 111–63. Available at:  
<http://search.ebscohost.com/login.aspx?direct=true&db=sih&AN=14956299&site=ehost-live>
- Spiegelhalter, D.J., Best, N.G., Carlin, B.P., Linde, A. van der (2002). Bayesian measures of model complexity and fit. *Journal of the Royal Statistical Society Series B (Statistical Methodology)*, 64, 583–639. Available at:  
<http://onlinelibrary.wiley.com/doi/10.1111/1467-9868.00353/abstract>
- Thomas, A., O’Hara, B., Ligges, U., Sturtz, S. (2006). Making BUGS open. *R News*, 6, 12–7. Available at: <http://cran.r-project.org/doc/Rnews/>.
- Wagenmakers, E.-J. (2007). A practical solution to the pervasive problems of  $p$  values. *Psychonomic Bulletin & Review*, 14, 779–804. Available at:  
<http://dx.doi.org/10.3758/BF03194105>

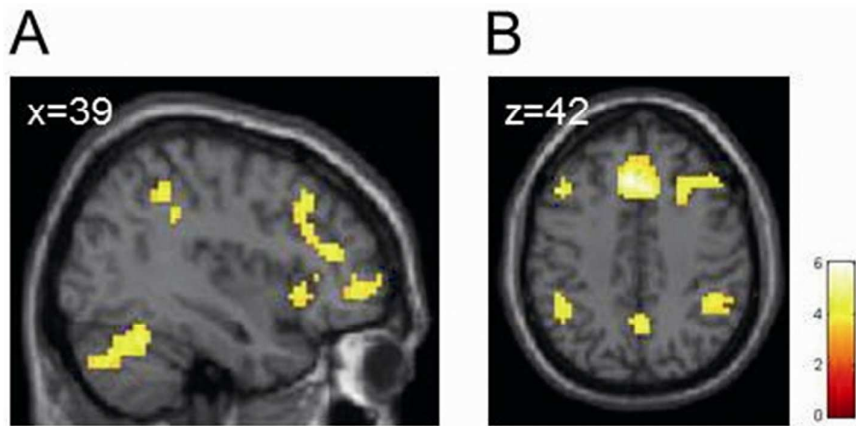


**Figure S1.** Neural correlates of subjective uncertainty during decision making. The decision-related activity of the anterior insular, parietal and frontal cortices increased with increasing subjective uncertainty.

Note:  $P < 0.001$ , uncorrected with a minimum cluster size of 20 voxels.

**Table S1.** Neural correlates of subjective uncertainty during decision making

Region	MNI centroid			No. of Voxel	Z value
	x	y	z		
Dorsomedial Prefrontal Cortex (DMPFC)	12	23	37	1368	4.74
Cerebellum	33	-61	-29	279	4.72
Inferior Frontal Gyrus / Precentral Gyrus	-48	41	1	644	4.65
Cerebellum	-27	-58	-32	647	4.51
Middle Temporal Gyrus	57	-40	1	110	4.31
Inferior Parietal Lobule	51	-46	22	146	4.24
Superior Temporal Gyrus	-54	-49	19	77	4.13
Superior Frontal Gyrus	-18	56	31	41	4.00
Thalamus	9	-13	13	24	3.89
Precuneus	3	-58	43	32	3.68
Inferior Parietal Lobule	-42	-52	43	76	3.63

*Note:*  $P < 0.001$ , uncorrected with a minimum cluster size of 20 voxels.